Original Paper

Cellular Physiology and Biochemistry

Cell Physiol Biochem 2007;20:45-54

Accepted: January 24, 2007

H_2O_2 Accelerates Cellular Senescence by Accumulation of Acetylated p53 via Decrease in the Function of SIRT1 by NAD^+ Depletion

Ayako Furukawa[1,2], Saeko Tada-Oikawa[1], Shosuke Kawanishi[1,3] and Shinji Oikawa[1]

[1]Department of Environmental and Molecular Medicine, Mie University Graduate School of Medicine, [2]JSPS Research Fellow, [3]Faculty of Health Science, Suzuka University of Medical Science

Key Words

SIRT1 • p53 • H_2O_2 • DNA damage • Cellular senescence • NAD^+

Abstract

It has been reported that p53 acetylation, which promotes cellular senescence, can be regulated by the NAD^+-dependent deacetylase SIRT1, the human homolog of yeast Sir2, a protein that modulates lifespan. To clarify the role of SIRT1 in cellular senescence induced by oxidative stress, we treated normal human diploid fibroblast TIG-3 cells with H_2O_2 and examined DNA cleavage, depletion of intracellular NAD^+, expression of p21, SIRT1, and acetylated p53, cell cycle arrest, and senescence-associated β-galactosidase (SA-β-gal) activity. DNA cleavage was observed immediately in TIG-3 cells treated with H_2O_2, though no cell death was observed. NAD^+ levels in TIG-3 cells treated with H_2O_2 were also decreased significantly. Pre-incubation with the poly (ADP-ribose) polymerase (PARP) inhibitor resulted in preservation of intracellular NAD^+ levels. The amount of acetylated p53 was increased in TIG-3 cells at 4h after H_2O_2 treatment, while there was little to no decrease in SIRT1 protein expression. The expression level of p21 was increased at 12h and continued to increase for up to 24h. Additionally, exposure of TIG-3 cells to H_2O_2 induced cell cycle arrest at 24h and increased SA-β-gal activity at 48h. This pathway likely plays an important role in the acceleration of cellular senescence by oxidative stress.

Introduction

Cellular senescence is a process by which cells irreversibly exit the cell cycle and cease to divide in response to a variety of stresses, including oxidative stress [1]. Oxidative stress damages DNA [1, 2], leading to activation of the tumor suppressor p53, a key regulator of the cell cycle and cellular senescence [3, 4]. Acetylation of p53 has been reported to promote the expression of growth suppressive genes [5] and to induce cellular senescence [3]. The NAD^+-dependent deacetylase SIRT1, the human homolog of the yeast Sir2 protein, regulates p53 activity via deacetylation [6-9]. Therefore, it is thought that SIRT1 may regulate cellular senescence through p53 [6, 9].

KARGER

Fax +41 61 306 12 34
E-Mail karger@karger.ch
www.karger.com

1015-8987/07/0204-0045$23.50/0

Accessible online at:
www.karger.com/cpb

Dr. Shinji Oikawa
Department of Environmental and Molecular Medicine
Mie University Graduate School of Medicine
2-174, Edobashi Tsu, Mie, 514-8507 (Japan)
Fax +81 59 231 5011, E-Mail s-oikawa@doc.medic.mie-u.ac.jp

DNA strand breaks induced by oxidative stress or topoisomerase inhibitors cause poly (ADP-ribose) polymerase (PARP) hyperactivation and subsequent NAD^+ depletion, leading to apoptosis [10, 11]. Sublethal H_2O_2 (< 0.45 mM) treatment of human fibroblasts caused growth arrest [4] and induced a senescent-like phenotype [12-14]. However, the role of DNA strand breaks induced by sublethal oxidative stress in cellular senescence is unknown.

To clarify the mechanism by which cellular senescence is induced by oxidative stress, we have now examined DNA cleavage, depletion of intracellular NAD^+, expression of p21, SIRT1, and acetylated p53, and cell cycle arrest in TIG-3 human embryonic lung fibroblasts treated with 150 μM H_2O_2. We also measured senescence-associated β-galactosidase (SA-β-gal) activity, a senescence biomarker [15], in TIG-3 cells treated with H_2O_2. We propose that sublethal concentrations of H_2O_2 (oxidative stress) induce cellular senescence via DNA strand breaks, PARP hyperactivation and subsequent NAD^+ depletion, decreased SIRT1 function, and the accumulation of acetylated p53 and induction of p21.

Materials and Methods

Cell culture and determination of cell viability

TIG-3 fibroblasts were obtained from the Health Science Research Resources Bank (Osaka, Japan) at a population doubling level (PDL) of 27. TIG-3 cells were grown in minimum essential medium (MEM) supplemented with 10% fetal calf serum (FCS) at 37°C under 5% CO_2 in a humidified atmosphere. Cells were incubated with different concentrations of H_2O_2 at 37°C for 1h; H_2O_2 was then removed from the culture and the cells were incubated in fresh culture medium containing 10% FCS for the indicated times. Cell viability was assessed using trypan blue dye exclusion and cell counting in a hemocytometer [16].

Detection of cellular DNA damage induced by H_2O_2

1.0 x 10^6 cells were incubated with 150 μM H_2O_2 at 37°C for the indicated times up to 1h. After 1h, H_2O_2 was removed from the culture and the cells were incubated in fresh culture medium containing 10% FCS for the indicated times. After incubation, cells were trypsinized and washed twice with phosphate buffered saline (PBS). Cell suspensions were solidified with agarose, followed by incubation with proteinase K as described previously [17]. Electrophoresis was performed using a pulsed field electrophoresis system (CHEF-DRII, Bio-Rad, Hercules, CA, USA) at 200 volts at 14°C. The switch time was 60sec for 15h followed by a 90sec switch time for 9h. The DNA in the gel was visualized using ethidium bromide.

Measurement of intracellular NAD^+ levels

1.0 x 10^6 cells were incubated with 150 μM H_2O_2 at 37°C for the indicated times up to 1h. After 1h, H_2O_2 was removed from the culture and the cells were incubated in fresh culture medium containing 10% FCS for the indicated times. Where indicated, cells were pre-incubated with 5 μM 4-amino-1, 8-naphthalimide (ANI) for 30min. Where indicated, cells were incubated with 10 mM NAD^+ and 150 μM H_2O_2 at 37°C for 1h, H_2O_2 was removed from the culture and the cells were incubated in fresh culture medium with 10 mM NAD^+. After incubation, cells were trypsinized and washed twice with PBS. Cell suspensions were extracted in cold 3 M perchloric acid and neutralized in 2 M KOH containing 0.3 N 3-(*N*-morpholino) propanesulfonic acid (MOPS). The intracellular NAD^+ levels were analyzed by HPLC with a Shimadzu photodiode array UV detector (SPD-M10A, Kyoto, Japan) as described previously [10]. Values were calibrated to standards and normalized to total protein. The protein content was determined by Bradford assay [18], using bovine serum albumin as standard.

SDS-PAGE and western blot analysis

1.0 x 10^5 cells were treated with 150 μM H_2O_2 for 1h, H_2O_2 was removed from the culture and the cells were incubated in fresh culture medium containing 10% FCS for the indicated times. Where indicated, cells were pre-incubated with 5 mM nicotinamide, 10 mM NAD^+ and 5 μM ANI for 30min. After incubation, cells were solubilized in gel sample buffer and boiled for 5min. Samples were separated on 4-20% polyacrylamide gels and transferred to polyvinylidene difluoride (PVDF) membranes. Membranes were blocked with 5% skim milk in Tris buffered saline (TBS) at 37°C for 1h and incubated in primary antibody for 1h at room temperature. After rinsing with TBS containing 0.1% polyoxyethylene sorbitan monolaurate (Tween-20) (TBS-T), membranes were incubated in horseradish peroxidase-conjugated secondary antibody (Santa Cruz Biochemical, Santa Cruz, CA, USA) at room temperature for 45min. After rinsing with TBS-T, membranes were exposed to the ECL Western Blotting Detection System (Amersham Biosciences, UK) for 1min. Anti-acetyl-p53 (Lys373 & 382) antibody and anti-SIRT1 (2G1/F7) antibody were purchased from Upstate Biotechnology (Lake Placid, NY, USA). Anti-p53 (DO-7) antibody was obtained from Novocastra Laboratories Ltd (Newcastle upon Tyne, UK). Anti-human actin (C-11) antibody and anti-p21 (187) antibody were purchased from Santa Cruz Biochemical (Santa Cruz, CA, USA). Human actin was used as a loading control.

RNA interference

Synthetic SIRT1 small interfering RNA (siRNA) was purchased from Takara Bio (Shiga, Japan). The 21-nt siRNA sequence targeting SIRT1 corresponded to the coding region 5'-GUA UUU ACG UUC AAA UGA ATT-3'. The scrambled control siRNA sequences were 5'-UUU GUG UUA CGC AAA UAA ATT-3' and 5'-UUU AUU UGC GUA ACA CAA ATT-3'. These siRNA were transfected into TIG-3 cells using TransIT-TKO (Mirus, Madison, WI, USA). After siRNA transfection for 24h, the cells were trypsinized and seeded in culture plate.

After incubation at 37°C for 48h, cells were subjected to analysis of western blot. After siRNA transfection for 24h, cells were pre-incubated with 10 mM NAD^+ or 5 μM ANI for 30min, followed by incubation with 150 μM H_2O_2 for 1h. Then, H_2O_2 was removed from the culture and the cells were incubated in fresh culture medium containing 10 mM NAD^+ or 5 μM ANI and 10% FCS for 23h. Total extracts were prepared and analyzed by SDS-PAGE and western blot analysis.

Real-time PCR

After the transfection of siRNA duplexes, total RNA was extracted with Trizol (Invitrogen, Carlsbad, CA, USA) and subjected to cDNA synthesis using a SYBR RT-PCR Kit (Perfect Real Time, Takara, Siga, Japan) with random primers. RT-PCR was carried out in 96-well plates, in a 25μl reaction volume containing 12.5μl of 2x SYBR Premix Ex *Taq* (Takara, Shiga, Japan), 2μl of cDNA, and 0.2 μM each of forward and reverse primers. The PCR was run on an iCycler (Bio-Rad, Hercules, CA, USA). The thermo-profile for SYBR real-time RT-PCR was 95°C for 10sec followed by 40 cycles of amplification, 95°C for 5sec, and 60°C for 20sec. The expression level of the SIRT1 gene was normalized to that of the β-actin gene.

Flow cytometric detection of cell cycle arrest by H_2O_2

1.0 x 10^6 cells were incubated with 150 μM H_2O_2 for 1h, H_2O_2 was removed from the culture and the cells were incubated in fresh culture medium containing 10% FCS for 23h. After incubation, cells were trypsinized and fixed with cold 70% ethanol at 4°C for 30min. Fixed cells were treated with 200μl of DNase-free RNase (0.5 mg/ml) at 37°C for 20min. After treatment, the cell pellets were resuspended in 500μl of propidium iodide (50 μg/ml) staining solution. The cells were incubated at 4°C for 10min in the dark and analyzed with a flow cytometer (FACScan, Becton Dickinson, San Jose, CA, USA) equipped with a single 488-nm argon laser. 2.0 x 10^4 cells per sample were acquired on FACScan and the data was analyzed using ModFit LT software (Verity Software House, Topsham, ME, USA).

SA-β-gal activity analysis

SA-β-gal activity was determined using a Senescence Detection Kit (Bio Vision, Palo Alto, CA, USA). 2.0 x 10^4 cells were incubated with 150 μM H_2O_2 for 1h, H_2O_2 was removed from the culture and the cells were incubated in fresh culture medium containing 10% FCS for 47h. Where indicated, TIG-3 cells were incubated with 10 mM NAD^+ or pre-incubated with 5 μM ANI. After H_2O_2 treatment, senescent cells were identified as blue-stained cells by standard light microscopy, and a total of 600 cells were counted in three random fields on a culture plate to determine the percentage of SA-β-gal positive cells.

2.0 x 10^4 cells were transiently transfected with 50 nM siRNA specific for SIRT1 or scrambled siRNA. After siRNA transfection for 24h, the cells were trypsinized and seeded in culture plates. After incubation at 37°C for 24h, cells were treated with 10 mM NAD^+ or 5 μM ANI for 30min, followed by incubation with 150 μM H_2O_2 for 1h at 37°C. Then, H_2O_2 was removed and the cells were incubated in fresh culture medium containing 10 mM NAD^+ or 5 μM ANI for 47h. After incubation, SA-β-gal activity was determined as described above.

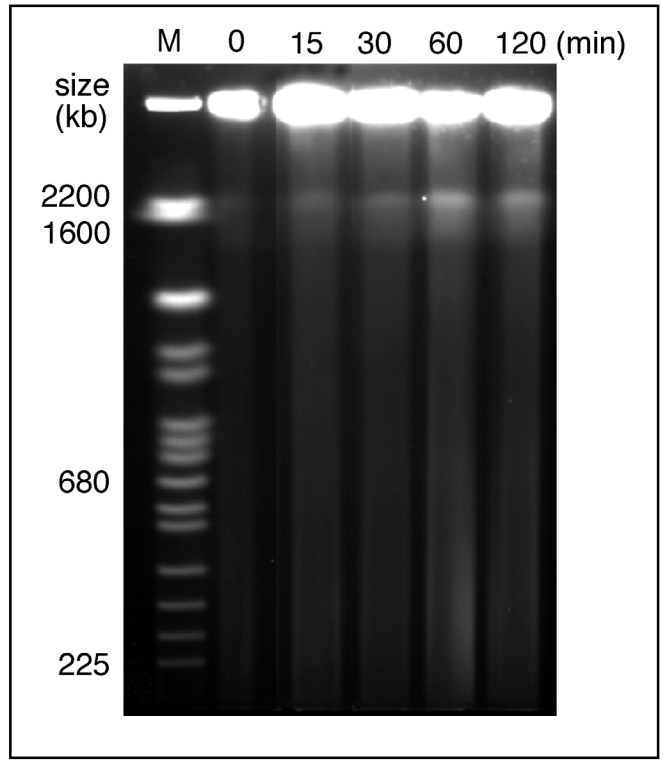

Fig. 1. Detection of intracellular DNA cleavage in TIG-3 cells treated with H_2O_2. 1.0 x 10^6 cells were treated with 150 μM H_2O_2 at 37°C for the indicated times up to 1h, H_2O_2 was removed from the culture and cells were maintained in fresh culture medium containing 10% FCS. Cells, prepared as agarose plugs, were lysed and subjected to pulsed field gel electrophoresis through a 1% agarose gel, as described in the Materials and Methods. The gel was stained with ethidium bromide. M: size marker DNA (*Saccharomyces cerevisiae*).

Results

DNA cleavage in TIG-3 cells treated with H_2O_2

We used the trypan blue exclusion test to determine cell viability and sublethal concentrations of H_2O_2. Treatment of TIG-3 cells with 150 μM H_2O_2 did not induce decreased cell viability, whereas treatment with 200 μM or greater concentrations of H_2O_2 caused decreased cell viability at 12h (data not shown). We next analyzed DNA cleavage in TIG-3 cells treated with sublethal 150 μM H_2O_2 using pulsed field gel electrophoresis. DNA fragments of 1-2 Mb appeared by 15min after addition of H_2O_2 and were present at greater quantities at 1 to 2h (Fig. 1).

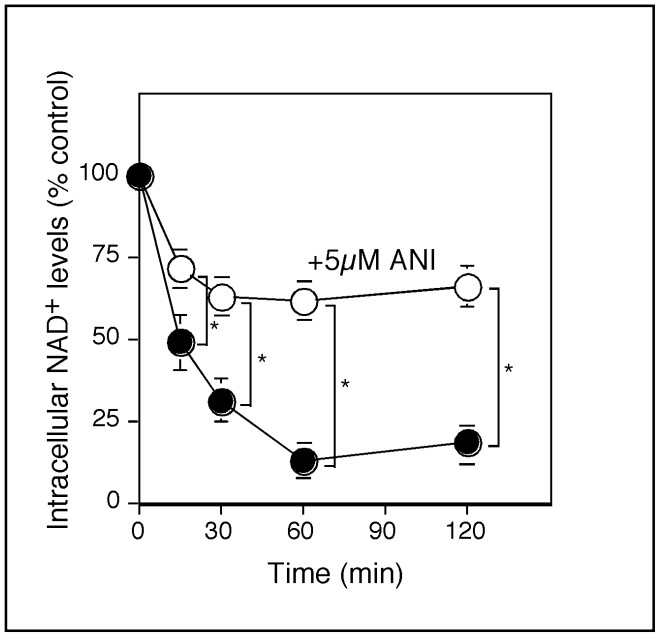

Fig. 2. Depletion of intracellular NAD^+ levels in TIG-3 cells treated with H_2O_2. 1.0 x 10^6 TIG-3 cells were treated with 150 μM H_2O_2 at 37°C for the indicated times up to 1h, H_2O_2 was removed from the culture and the cells were maintained in fresh culture medium containing 10% FCS. Where indicated, cells were pre-incubated with 5 μM ANI for 30min. Following cell lysis, NAD^+ was extracted and analyzed as described in the Materials and Methods. Results represent means ± SE of five independent experiments. Asterisks indicate statistically significant differences of sample values upon addition of ANI. (*, $P < 0.01$).

Depletion of intracellular NAD^+ levels in TIG-3 cells treated with H_2O_2

DNA damage can lead to PARP activation followed by reduced levels of NAD^+, a PARP substrate [10, 11]. To determine whether DNA damage induced by 150 μM H_2O_2 causes depletion of NAD^+, we analyzed intracellular NAD^+ levels in TIG-3 cells. Intracellular NAD^+ levels were decreased significantly by 15min and continued to decrease for up to 1h (Fig. 2). The depletion of intracellular NAD^+ levels induced by 150 μM H_2O_2 treatment was significantly inhibited by the addition of ANI, a PARP inhibitor (Fig. 2). Furthermore, intracellular NAD^+ levels were restored to normal levels at 12h after the addition of H_2O_2, and were maintained at normal levels for up to 48h (data not shown).

Increased expression of p21 and acetylated p53 in H_2O_2 treated TIG-3 cells

A) Accumulation of p21 and acetylated p53 in TIG-3 cells treated with H_2O_2. To examine alterations in expression of acetylated p53 and SIRT1 in TIG-3 cells treated with 150 μM H_2O_2, we performed SDS-PAGE and western blotting. The expression of acetylated p53 increased by 4h and continued to increase for up to 24h, while p53 expression increased up to 12h (Fig. 3A). The expression of p21, which is a transcriptional target of p53, was increased at 12h and continued to increase for up to 24h. SIRT1 expression was little changed by treatment with 150 μM H_2O_2 (Fig. 3A). In addition, H_2O_2-induced p53 acetylation was decreased by NAD^+ supplementation and pretreatment with ANI (Fig. 3B). On the other hand, p53 acetylation was increased by the addition of nicotinamide, a SIRT1 inhibitor (Fig. 3B).

B) Accumulation of acetylated p53 following SIRT1 siRNA treatment. Accumulation of acetylated p53 by inhibition of SIRT1 deacetylase function was confirmed using siRNA. We performed RT-PCR to evaluate the depletion of SIRT1 mRNA by siRNA. Transfection of TIG-3 cells with SIRT1 siRNA reduced endogenous SIRT1 mRNA levels by 60% in comparison to the levels in control cells (Fig. 3E). Following the transfection of SIRT1 siRNA, western blot analysis with an anti-SIRT1 antibody demonstrated a reduction in endogenous SIRT1 expression (Fig. 3C). Acetylated p53 accumulated after SIRT1 siRNA transfection in TIG-3 cells (Fig. 3C), suggesting that SIRT1 inhibition increased the amount of acetylated p53. Furthermore, NAD^+ supplementation and pretreatment with ANI did not inhibit H_2O_2-induced p53 acetylation in TIG-3 cells transfected with SIRT1 siRNA (Fig. 3D). Similar results were obtained in TIG-3 cells treated with nicotinamide (Fig. 3D).

H_2O_2 treatment induces cell cycle arrest in TIG-3 cells

To confirm the features of senescence, cell cycle distribution was analyzed in H_2O_2 treated TIG-3 cells. As compared to control cells, 150 μM H_2O_2 increased the population of G1 phase cells from 52.9±0.52% to 69.0±1.23% and decreased the population of S phase cells from 32.7±0.29% to 15.4±3.04% at 24h after treatment (Fig. 4). These results suggest that 150 μM H_2O_2 inhibited cell cycle progression at the G1 phase.

H_2O_2 treatment results in the appearance of SA-β-gal activity in TIG-3 cells

We measured SA-β-gal activity, a senescence biomarker, in TIG-3 cells treated with 150 μM H_2O_2. 48h after the addition of H_2O_2, 79.4±12.2% of treated cells were SA-β-gal positive (Fig. 5B and E), whereas

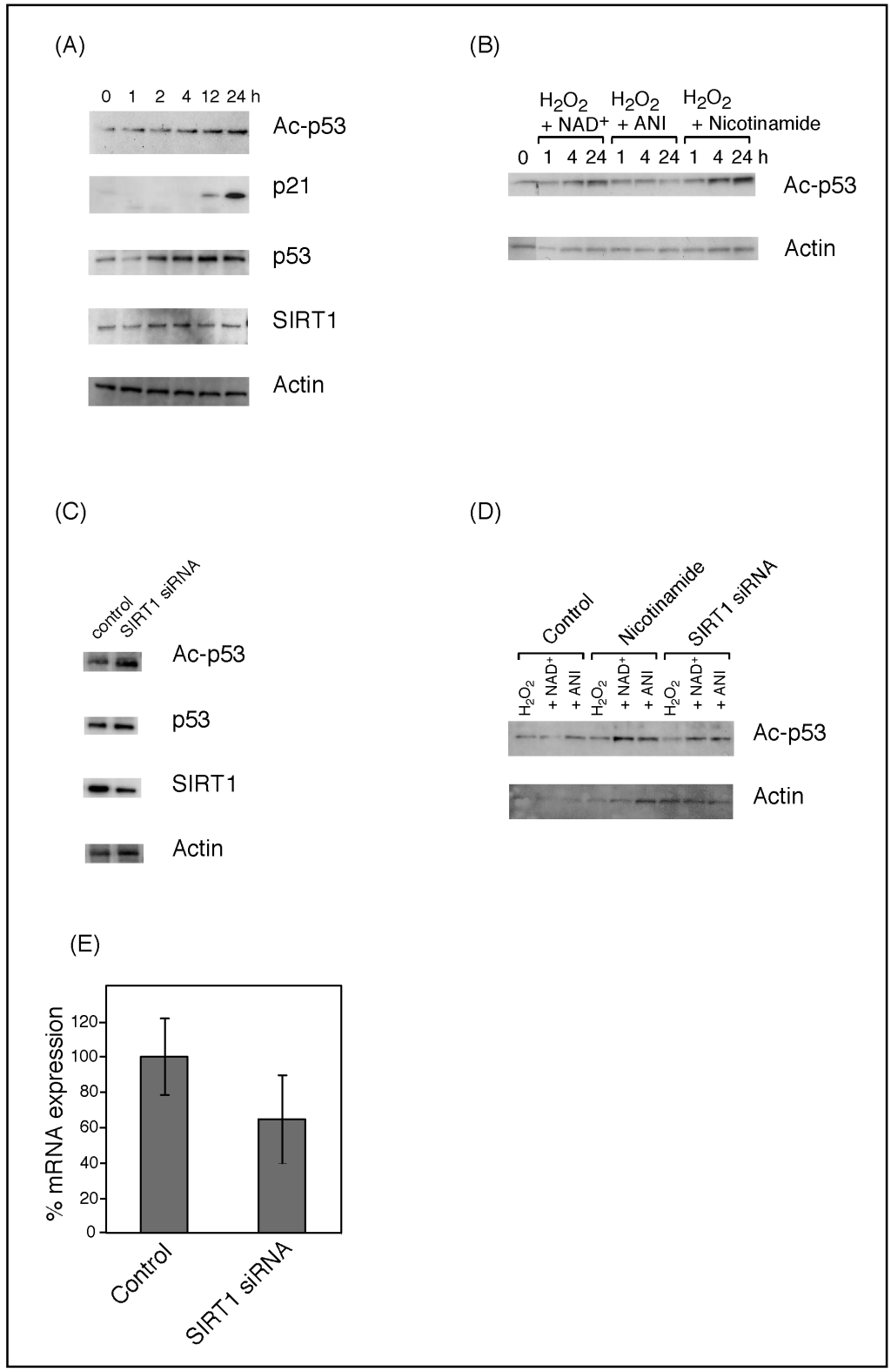

Fig. 3. Accumulation of acetylated p53 in TIG-3 cells. (A) 1.0 x 10^5 TIG-3 cells were treated with 150 μM H_2O_2 at 37°C for 1h, H_2O_2 was removed from the culture and the cells were incubated in fresh culture medium containing 10% FCS for the indicated times. After incubation, cells were analyzed by 4-20% SDS-PAGE and western blots were performed using anti-acetyl-p53 (Lys373 & 382), anti-SIRT1 (2G1/F7), anti-p21 (187), anti-p53 (DO-7), and anti-human actin (C-11) antibodies as described in the Materials and Methods. (B) 1.0 x 10^5 TIG-3 cells were pretreated with 10 mM NAD^+, 5 μM ANI or 5 mM nicotinamide for 30min, followed by incubation with 150 μM H_2O_2 for 1h at 37°C. After incubation, H_2O_2 was removed from the culture and the cells were incubated in fresh culture medium containing 10 mM NAD^+ or 5 μM ANI and 10% FCS for the indicated times. Total extracts were prepared and analyzed by SDS-PAGE and western blots as described in the Materials and Methods. (C) TIG-3 cells were transiently transfected with 25 nM siRNA specific for SIRT1. Total extracts were prepared and analyzed by SDS-PAGE and western blots as described in the Materials and Methods. (D) TIG-3 cells were transiently transfected with 50 nM siRNA specific for SIRT1. After 24h, transfected cells were pretreated with 10 mM NAD^+ or 5 μM ANI for 30min at 37°C, followed by incubation with 150 μM H_2O_2 for 1h at 37°C. TIG-3 cells were pretreated with 5 mM nicotinamide, and 10 mM NAD^+ or 5 μM ANI for 30min at 37°C, followed by incubation with 150 μM H_2O_2 for 1h at 37°C. Then, H_2O_2 was removed and the cells were incubated in fresh culture medium containing 10 mM NAD^+ or 5 μM ANI and 10% FCS for 23h. Total extracts were prepared and analyzed by SDS-PAGE and western blots as described in the Materials and Methods. (E) Quantitative real-time RT-PCR was used to assess SIRT1 mRNA levels and β-actin was used to normalize mRNA concentration.

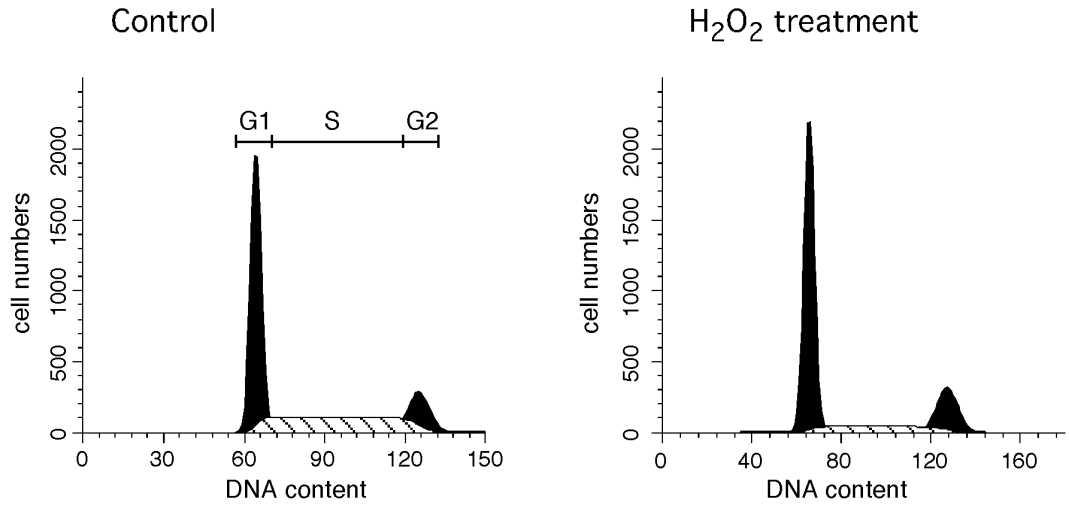

	G1 (%)	G2/M (%)	S (%)
control	52.9±0.52	14.4±0.67	32.7±0.29
H_2O_2 treatment	69.0±1.23*	14.7±0.41	15.4±3.04*

Fig. 4. Effect of H_2O_2 treatment on cell cycle distribution in TIG-3 cells. 1.0 x 10^6 TIG-3 cells were treated with 150 μM H_2O_2 for 1h, H_2O_2 was removed and the cells were incubated in fresh culture medium containing 10% FCS for 23h. After incubation, cell cycle distribution was analyzed by flow cytometry. The values are representative of three independent experiments expressed as mean±SD. *P<0.05, compared with the control.

1.7±1.2% of control cells were SA-β-gal positive (Fig. 5A and E). In addition, we investigated whether the addition of exogenous NAD^+ could prevent H_2O_2-accelerated cellular senescence. Addition of 10 mM NAD^+ to the culture medium prevented the depletion of NAD^+ in H_2O_2 treated TIG-3 cells (Fig. 5G). Previous reports have indicated that human diploid fibroblasts express membrane channels that can bind and transport extracellular NAD^+ into the cell [19]. NAD^+ supplementation reduced the number of SA-β-gal positive cells (21.1±8.2%) following H_2O_2 treatment (Fig. 5C and E). Pretreatment of TIG-3 cells with ANI also reduced the number of SA-β-gal positive cells (50.5±2.9%) following addition of H_2O_2 (Fig. 5D and E). However, H_2O_2-mediated SA-β-gal positive cells were not reduced by NAD^+ supplementation or ANI treatment in TIG-3 cells transfected with SIRT1 siRNA or treated with nicotinamide (Fig. 5F). In contrast, SA-β-gal positive cells were reduced by NAD^+ supplementation or ANI treatment in TIG-3 cells transfected with scrambled siRNA (Fig. 5F).

Discussion

In this study, we report that 150 μM H_2O_2 induced DNA cleavage in TIG-3 cells at 15min, although this concentration of H_2O_2 had no effect on cell viability. It is well known that PARP is rapidly activated by DNA damage [20, 21] and consumes NAD^+ to modify specific acceptor proteins with poly(ADP-ribose) [22, 23]. We measured the levels of intracellular NAD^+, which is required for SIRT1 deacetylase activity *in vivo*, in TIG-3 cells treated with 150 μM H_2O_2. NAD^+ levels were decreased by over 50% after H_2O_2 treatment for 15min and continued to decrease for up to 1h. The depletion of

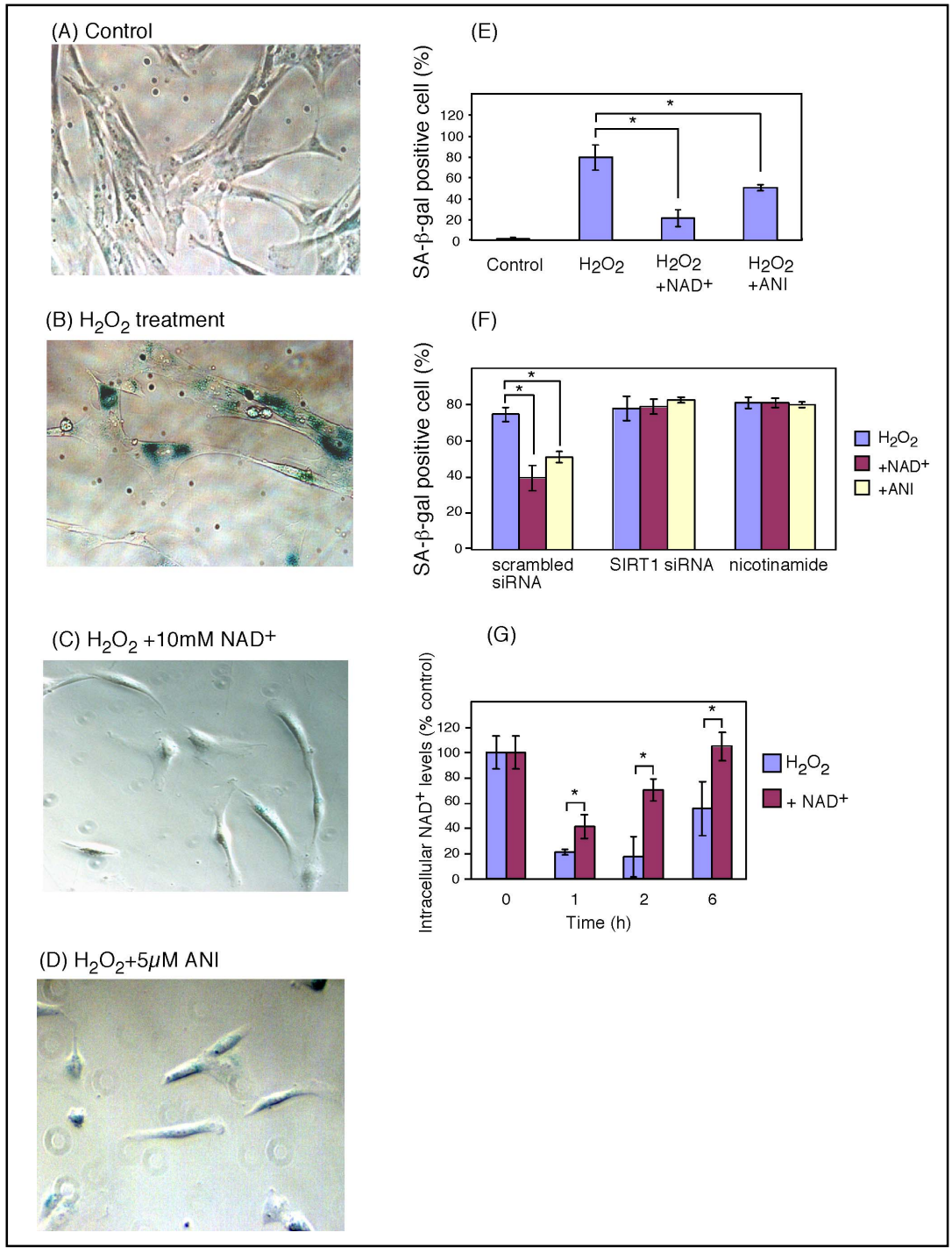

Fig. 5. SA-β-gal activity of human TIG-3 cells treated with H_2O_2. (A, B) 2.0 x 10^4 TIG-3 cells were treated with (B) or without (A) 150 μM H_2O_2 at 37°C for 1h, H_2O_2 was removed from the culture and the cells were maintained in fresh culture medium containing 10% FCS for 47h. After incubation, SA-β-gal activity was determined as described in Materials and Methods. (C) Cells were treated with 150 μM H_2O_2 and 10 mM NAD^+ at 37°C for 1h, H_2O_2 was removed from the culture and the cells were maintained in fresh culture medium containing 10 mM NAD^+ and10% FCS for 47 h. (D) Cells were pretreated with 5 μM ANI for 30min and treated with 150 μM H_2O_2 for 1h. After H_2O_2 treatment, H_2O_2 was removed from the culture and the cells were maintained in fresh culture medium containing 5 μM ANI and 10% FCS for 47h. (E) The percentages of SA-β-gal positive cells were determined and are presented in E as mean±SD (n=3). *P<0.05, compared with the H_2O_2 treatment. (F) 'SIRT1 siRNA or scrambled siRNA': TIG-3 cells were transiently transfected with 50 nM siRNA specific for SIRT1 or 50 nM scrambled siRNA. After 24h, transfected cells were pretreated with 10 mM NAD^+ or 5 μM ANI for 30min at 37°C, followed by incubation with 150 μM H_2O_2 for 1h at 37°C. Then, H_2O_2 was removed and the cells were incubated in fresh culture medium containing 10 mM NAD^+ or 5 μM ANI and 10% FCS for 47h. 'Nicotinamide': TIG-3 cells were pretreated with 5 mM nicotinamide, and 10 mM NAD^+ or 5 μM ANI for 30min at 37°C, followed by incubation with 150 μM H_2O_2 for 1h at 37°C. Then, H_2O_2 was removed and the cells were incubated in fresh culture medium containing 5 mM nicotinamide, and 10 mM NAD^+ or 5 μM ANI and 10% FCS for 47h. After incubation, SA-β-gal activity was determined as described in the Materials and Methods. *P<0.05, compared with the H_2O_2 treatment. (G) 1.0 x 10^6 cells were incubated with 10 mM NAD^+ and 150 μM H_2O_2 at 37°C for 1h, H_2O_2 was removed from the culture and the cells were incubated in fresh culture medium containing 10 mM NAD^+ and 10% FCS for 47h. NAD^+ levels were analyzed as described in the Materials and Methods. *P<0.05, compared with the H_2O_2 treatment.

NAD^+ was prevented by pre-incubation with a PARP inhibitor, ANI. These results suggest that NAD^+ depletion in H_2O_2-treated TIG-3 cells is caused by PARP activation in response to DNA damage.

It has been reported that NAD^+ depletion in response to PARP activation leads to apoptosis-inducing factor (AIF) translocation from mitochondria to nuclei, resulting in programmed cell death [20, 21, 24]. Our experimental conditions did not induce AIF translocation into the nucleus (data not shown). Thus, since it is thought that hyperactivation of PARP in response to oxidative DNA damage can decrease SIRT1 deacetylase function through NAD^+ depletion, we examined alterations in the expression of acetylated p53, a SIRT1 substrate. The amount of acetylated p53 was increased following 150 μM H_2O_2 treatment, although SIRT1 expression was little changed. In addition, NAD^+ supplementation and a PARP inhibitor ANI decreased the amount of acetylated p53 in TIG-3 cells treated with H_2O_2. On the other hand, nicotinamide treatment increased H_2O_2-induced p53 acetylation. Therefore, it is considered that NAD^+ depletion plays an important role in p53 deacetylation by SIRT1. Furthermore, we have confirmed that SIRT1 siRNA treatment increases the amount of acetylated p53 in TIG-3 cells. NAD^+ supplementation and pretreatment with ANI did not reduce H_2O_2-induced p53 acetylation in TIG-3 cells transfected with SIRT1 siRNA and treated with nicotinamide, suggesting that SIRT1 regulated p53 deacetylation.

Some recent papers have reported that although SIRT1 deacetylates p53, this does not play a role in cell survival following DNA damage in certain cell lines [25-27]. Thus, since p53 is directly involved in G1 arrest through the induction of p21 [28], we assessed p21 expression in TIG-3 cells treated with 150 μM H_2O_2, showing that p21 expression correlated with increased levels of p53 acetylation. Furthermore, we demonstrated that 150 μM H_2O_2 induced cell cycle arrest in G1 phase at 24h and increased SA-β-gal activity at 48h in TIG-3 cells. Interestingly, the addition of 10 mM NAD^+ to the culture medium significantly reduced H_2O_2-mediated SA-β-gal activity. In addition, a PARP inhibitor ANI also reduced SA-β-gal activity in TIG-3 cells treated with H_2O_2. In contrast, NAD^+ supplementation and ANI treatment did not reduce SA-β-gal activity in TIG-3 cells treated with nicotinamide or transfected with SIRT1 siRNA. Therefore, we conclude that sublethal concentrations (150 μM) of H_2O_2 can accelerate cellular senescence by causing the accumulation of acetylated p53 via NAD^+ depletion and decreased SIRT1 deacetylase function.

Numerous studies of SIRT1 function have been performed in mammalian cells and animals [29, 30]. For instance, treatment of human breast and lung cancer cells with sirtinol, a SIRT1 inhibitor, has been found to induce a senescence-like growth arrest [31]. The loss of SIRT1 with age was accelerated in mice with accelerated aging, but was not observed in a long-lived mouse [32]. Furthermore, it has been reported that SIRT1-null mice are viable, but most of them die during the early postnatal period [27, 33]. Therefore, our results and several other reports [30, 34-37] are consistent with the idea that p53 deacetylation by SIRT1 regulates important cellular processes, including cellular senescence. However, Alt's group showed that SIRT1-deficient ($SIRT1^{-/-}$) mouse embryonic fibroblasts (MEFs) have enhanced proliferative capacity and fail to enter senescence under conditions of chronic oxidative stress [38]. In addition, nicotinamide, a SIRT1 inhibitor, has been reported to extend the replicative life span of primary human fibroblasts [39]. Collectively, although it remains unclear whether SIRT1 directly regulates lifespan, SIRT1 may contribute to cellular senescence in mammalian cells.

We have previously reported that oxidative stress induces DNA damage in telomere sequences as well as telomere shortening [40-44]. In addition, we have demonstrated that the level of carbonylated proteins, an indicator of oxidative damage to proteins, increased in senescence-accelerated prone mouse strain 8, which displayed deterioration in learning and memory, as compared to control mice [45]. It has been reported that cellular senescence may occur if DNA damage is not serious enough to induce cell death, but cannot be completely repaired [46]. Thus, oxidative stress-induced DNA damage plays a key role in cellular senescence. In this study, we have demonstrated a pathway of oxidative stress-mediated cellular senescence: DNA cleavage by sublethal concentrations of H_2O_2 induces PARP hyperactivation and subsequent NAD^+ depletion, followed by decreased SIRT1 function and the accumulation of acetylated p53 and transcription of p53 target genes. This pathway is likely to play an important role in cellular senescence caused by oxidative stress.

Acknowledgements

This work was supported by a Grant-in-Aid from the Ministry of Education, Culture, Sports, Science and Technology of Japan.

References

1 Ben-Porath I, Weinberg RA: The signals and pathways activating cellular senescence. Int J Biochem Cell Biol 2005;37:961-976.

2 Harman D: Aging: A theory based on free radical and radiation chemistry. J Gerontol 1956;11:298-300.

3 Bond J, Haughton M, Blaydes J, Gire V, Wynford-Thomas D, Wyllie F: Evidence that transcriptional activation by p53 plays a direct role in the induction of cellular senescence. Oncogene 1996;13:2097-2104.

4 Wang Y, Meng A, Zhou D: Inhibition of phosphatidylinostol 3-kinase uncouples H_2O_2-induced senescent phenotype and cell cycle arrest in normal human diploid fibroblasts. Exp Cell Res 2004;298:188-196.

5 Luo J, Li M, Tang Y, Laszkowska M, Roeder RG, Gu W: Acetylation of p53 augments its site-specific DNA binding both in vitro and in vivo. Proc Natl Acad Sci U S A 2004;101:2259-2264.

6 Langley E, Pearson M, Faretta M, Bauer UM, Frye RA, Minucci S, Pelicci PG, Kouzarides T: Human SIR2 deacetylates p53 and antagonizes PML/p53-induced cellular senescence. EMBO J 2002;21:2383-2396.

7 Luo J, Nikolaev AY, Imai S, Chen D, Su F, Shiloh A, Guarente L, Gu W: Negative control of p53 by Sir2alpha promotes cell survival under stress. Cell 2001;107:137-148.

8 Vaziri H, Dessain SK, Ng Eaton E, Imai SI, Frye RA, Pandita TK, Guarente L, Weinberg RA: hSIR2(sirt1) functions as an NAD-dependent p53 deacetylase. Cell 2001;107:149-159.

9 Smith J: Human Sir2 and the 'silencing' of p53 activity. Trends Cell Biol 2002;12:404-406.

10 Mizutani H, Tada-Oikawa S, Hiraku Y, Oikawa S, Kojima M, Kawanishi S: Mechanism of apoptosis induced by a new topoisomerase inhibitor through the generation of hydrogen peroxide. J Biol Chem 2002;277:30684-30689.

11 Szabo C, Dawson VL: Role of poly(ADP-ribose) synthetase in inflammation and ischaemia-reperfusion. Trends Pharmacol Sci 1998;19:287-298.

12 Chen Q, Ames BN: Senescence-like growth arrest induced by hydrogen peroxide in human diploid fibroblast F65 cells. Proc Natl Acad Sci U S A 1994;91:4130-4134.

13 Dumont P, Burton M, Chen QM, Gonos ES, Frippiat C, Mazarati JB, Eliaers F, Remacle J, Toussaint O: Induction of replicative senescence biomarkers by sublethal oxidative stresses in normal human fibroblast. Free Radic Biol Med 2000;28:361-373.

14 Dumont P, Royer V, Pascal T, Dierick JF, Chainiaux F, Frippiat C, de Magalhaes JP, Eliaers F, Remacle J, Toussaint O: Growth kinetics rather than stress accelerate telomere shortening in cultures of human diploid fibroblasts in oxidative stress-induced premature senescence. FEBS Lett 2001;502:109-112.

15 Dimri GP, Lee X, Basile G, Acosta M, Scott G, Roskelley C, Medrano EE, Linskens M, Rubelj I, Pereira-Smith O, Peacocke M, Campisi J: A biomarker that identifies senescent human cells in culture and in aging skin in vivo. Proc Natl Acad Sci U S A 1995;92:9363-9367.

16 Hiraku Y, Kawanishi S: Involvement of oxidative DNA damage and apoptosis in antitumor actions of aminosugars. Free Radic Res 1999;31:389-403.

17 Ito K, Yamamoto K, Kawanishi S: Manganese-mediated oxidative damage of cellular and isolated DNA by isoniazid and related hydrazines: Non-fenton-type hydroxyl radical formation. Biochemistry 1992;31:11606-11613.

18 Bradford MM: A rapid and sensitive method for the quantitation of microgram quantities of protein utilizing the principle of protein-dye binding. Anal Biochem 1976;72:248-254.

19 Dilley TK, Bowden GT, Chen QM: Novel mechanisms of sublethal oxidant toxicity: Induction of premature senescence in human fibroblasts confers tumor promoter activity. Exp Cell Res 2003;290:38-48.

20 Kolthur-Seetharam U, Dantzer F, McBurney MW, de Murcia G, Sassone-Corsi P: Control of AIF-mediated cell death by the functional interplay of SIRT1 and PARP-1 in response to DNA damage. Cell Cycle 2006;5:873-877.

21 Yu SW, Wang H, Poitras MF, Coombs C, Bowers WJ, Federoff HJ, Poirier GG, Dawson TM, Dawson VL: Mediation of poly(ADP-ribose) polymerase-1-dependent cell death by apoptosis-inducing factor. Science 2002;297:259-263.

22 Virag L, Szabo C: The therapeutic potential of poly(ADP-ribose) polymerase inhibitors. Pharmacol Rev 2002;54:375-429.

23 D'Amours D, Desnoyers S, D'Silva I, Poirier GG: Poly(ADP-ribosyl)ation reactions in the regulation of nuclear functions. Biochem J 1999;342 (Pt 2):249-268.

24 Pillai JB, Isbatan A, Imai S, Gupta MP: Poly(ADP-ribose) polymerase-1-dependent cardiac myocyte cell death during heart failure is mediated by NAD^+ depletion and reduced Sir2alpha deacetylase activity. J Biol Chem 2005;280:43121-43130.

25 Solomon JM, Pasupuleti R, Xu L, McDonagh T, Curtis R, DiStefano PS, Huber LJ: Inhibition of SirT1 catalytic activity increases p53 acetylation but does not alter cell survival following DNA damage. Mol Cell Biol 2006;26:28-38.

26 Kamel C, Abrol M, Jardine K, He X, McBurney MW: SirT1 fails to affect p53-mediated biological functions. Aging Cell 2006;5:81-88.

27 Cheng HL, Mostoslavsky R, Saito S, Manis JP, Gu Y, Patel P, Bronson R, Appella E, Alt FW, Chua KF: Developmental defects and p53 hyperacetylation in Sir2 homolog (SIRT1)-deficient mice. Proc Natl Acad Sci U S A 2003;100:10794-10799.

28 Herbig U, Sedivy JM: Regulation of growth arrest in senescence: Telomere damage is not the end of the story. Mech Ageing Dev 2006;127:16-24.

29 Longo VD, Kennedy BK: Sirtuins in aging and age-related disease. Cell 2006;126:257-268.

30 Leibiger IB, Berggren PO: Sirt1: A metabolic master switch that modulates lifespan. Nat Med 2006;12:34-36.

31 Ota H, Tokunaga E, Chang K, Hikasa M, Iijima K, Eto M, Kozaki K, Akishita M, Ouchi Y, Kaneki M: Sirt1 inhibitor, sirtinol, induces senescence-like growth arrest with attenuated Ras-MAPK signaling in human cancer cells. Oncogene 2006;25:176-185.

32 Sasaki T, Maier B, Bartke A, Scrable H: Progressive loss of SIRT1 with cell cycle withdrawal. Aging Cell 2006;5:413-422.

33 McBurney MW, Yang X, Jardine K, Hixon M, Boekelheide K, Webb JR, Lansdorp PM, Lemieux M: The mammalian SIR2alpha protein has a role in embryogenesis and gametogenesis. Mol Cell Biol 2003;23:38-54.

34 Kume S, Haneda M, Kanasaki K, Sugimoto T, Araki S, Isono M, Isshiki K, Uzu T, Kashiwagi A, Koya D: Silent information regulator 2 (SIRT1) attenuates oxidative stress-induced mesangial cell apoptosis via p53 deacetylation. Free Radic Biol Med 2006;40:2175-2182.

35 Kruszewski M, Szumiel I: Sirtuins (histone deacetylases III) in the cellular response to DNA damage-facts and hypotheses. DNA Repair 2005;4:1306-1313.

36 Lim CS: SIRT1: Tumor promoter or tumor suppressor? Med Hypotheses 2006;67:341-344.

37 Zhang J: Are poly(ADP-ribosyl)ation by PARP-1 and deacetylation by Sir2 linked? Bioessays 2003;25:808-814.

38 Chua KF, Mostoslavsky R, Lombard DB, Pang WW, Saito S, Franco S, Kaushal D, Cheng HL, Fischer MR, Stokes N, Murphy MM, Appella E, Alt FW: Mammalian SIRT1 limits replicative life span in response to chronic genotoxic stress. Cell Metab 2005;2:67-76.
39 Lim CS, Potts M, Helm RF: Nicotinamide extends the replicative life span of primary human cells. Mech Ageing Dev 2006;127:511-514.
40 Oikawa S, Kawanishi S: Site-specific DNA damage at GGG sequence by oxidative stress may accelerate telomere shortening. FEBS Lett 1999;453:365-368.
41 Oikawa S, Tada-Oikawa S, Kawanishi S: Site-specific DNA damage at the GGG sequence by UVA involves acceleration of telomere shortening. Biochemistry 2001;40:4763-4768.
42 Kawanishi S, Hiraku Y, Oikawa S: Mechanism of guanine-specific DNA damage by oxidative stress and its role in carcinogenesis and aging. Mutat Res 2001;488:65-76.
43 Kawanishi S, Oikawa S: Mechanism of telomere shortening by oxidative stress. Ann N Y Acad Sci 2004;1019:278-284.
44 Jun ES, Lee TH, Cho HH, Suh SY, Jung JS: Expression of telomerase extends longevity and enhances differentiation in human adipose tissue-derived stromal cells. Cell Physiol Biochem 2004;14:261-268.
45 Nabeshi H, Oikawa S, Inoue S, Nishino K, Kawanishi S: Proteomic analysis for protein carbonyl as an indicator of oxidative damage in senescence-accelerated mice. Free Radic Res 2006;40:1173-1181.
46 Beckman KB, Ames BN: The free radical theory of aging matures. Physiol Rev 1998;78:547-581.